

# Zebrafish Neurolin-a and -b, Orthologs of ALCAM, Are Involved in Retinal Ganglion Cell Differentiation and Retinal Axon Pathfinding

HEIKE DIEKMANN AND CLAUDIA A.O. STUERMER\*

Department of Biology, Universität Konstanz, 78578 Konstanz, Germany

## ABSTRACT

Neurolin-a and Neurolin-b (also called *alcam* and *nlcam*, respectively) are zebrafish orthologs of human ALCAM, an adhesion protein of the immunoglobulin superfamily with functions in axon growth and guidance. Within the developing zebrafish retina, onset and progression of Neurolin-a expression parallels the pattern of retinal ganglion cell (RGC) differentiation. By using a morpholino-based knockdown approach, we show that Neurolin-a (but not Neurolin-b) is necessary for a crucial step in RGC differentiation. Without Neurolin-a, a large proportion of

RGCs fail to develop, and RGC axons are absent or reduced in number. Subsequently, Neurolin-a is required for RGC survival and for the differentiation of all other retinal neurons. Neurolin-b is expressed later in well-differentiated RGCs and is required for RGC axon pathfinding. Without Neurolin-b, RGC axons grow in highly aberrant routes along the optic tract and/or fail to reach the optic tectum. Thus, the zebrafish Neurolin paralogs are involved in distinct steps of retinotectal development.

Indexing terms: zebrafish retinotectal system; morpholino knockdown; gene duplication

The visual system has been widely employed to investigate the cellular and molecular mechanisms that regulate neural cell-fate determination and control the specification of neuronal connections (Livesey and Cepko, 2001; Dingwell et al., 2000; Yamagata and Sanes, 2005). Recent findings suggest that retinal progenitors go through a series of changes in intrinsic properties (such as expression of specific transcription factors) that control their competence to generate different cell types, whereas extrinsic cues act to influence the ratios of the cell types that are produced (Cepko, 1999). Steps during retinal ganglion cell (RGC) differentiation include expression of the basic helix-loop-helix (bHLH) transcription factor *atoh7* (*atoh7*) and the diffusible morphogen sonic hedgehog (*shh*) (Masai et al., 2000; Neumann and Nüsslein-Volhardt, 2000). In addition, expression of cell surface proteins promotes communication between neighboring cells and the environment and provides outgrowing axons with appropriate receptors for guidance cues (Stuermer and Bastmeyer, 2000; Laessing and Stuermer, 1996). Growing axons are guided by long-range, diffusible guidance molecules and short-range recognition proteins that collectively promote the establishment of connections between the retina and the optic tectum (Dickson, 2002). In this context, membrane proteins of the immunoglobulin superfamily (IgSF) have been implicated in numerous adhesive and signaling interactions (Rougon and Hobert, 2003), functioning as growth and guidance receptors (Deiner et al., 1997; Stuermer and Bastmeyer, 2000).

The IgSF molecule Neurolin/ALCAM consists of five extracellular Ig-like domains, a transmembrane, and a short intracellular portion (Paschke et al., 1992; Laessing et al., 1994). In fish, Neurolin (also *alcam* or *zf DM-GRASP*; Kanki et al., 1994) is expressed on developing axons in defined neuronal subsystems and is functionally involved in the growth and guidance of secondary motoneurons (Fashena and Westerfield, 1999; Ott et al., 2001) and RGC axons (Ott et al., 1997; Leppert et al., 1999; for review, see Stuermer and Bastmeyer, 2000). Repeated injections of Neurolin antibodies into the eyes of growing goldfish has been shown to affect the growth behavior of Neurolin-expressing axons from newborn RGCs at the retinal margin (Ott et al., 1997; Leppert et al., 1999). Affected axons fail to reach the optic disc, but turn around and grow in circles or in various other abnormal routes. Therefore, Neurolin is involved in intraretinal pathfinding in the goldfish eye. In

---

Grant sponsor: Deutsche Forschungsgemeinschaft (DFG); Grant numbers: Stu 112/17-3 and TR SFB 11 (to C.A.O.S.). Dr. Diekmann's current address: Summit plc, 91 Milton Park, Abingdon, OX14 4RY, UK.

\*Correspondence to: Claudia A.O. Stuermer, Department of Biology, Universität Konstanz, 78578 Konstanz, Germany.  
E-mail: claudia.stuermer@uni-konstanz.de

young neurons, Neurolin is expressed all along RGC axons, whereas in mature neurons Neurolin is found only at RGC cell contact sites and synapses (Paschke et al., 1992). This suggests a function for Neurolin in RGC cell-cell communication (Fashena and Westerfield, 1995) and signal transduction in addition to axon guidance. However, this hypothesis has so far not been addressed in vivo. Therefore, we decided to analyze the physiological function of Neurolin during retina development in the zebrafish, a model organism for developmental biology.

Here we describe the identification of a second *neurolin* gene in zebrafish, *neurolin-b*. Gene duplication is thought to play an important role in evolution by providing new genetic material for selection, which might be followed by partitioning of gene function (Ohno, 1999). The two paralogs, *neurolin-a* and *neurolin-b*, show overlapping but distinct expression patterns suggesting subfunctionalization. By using a morpholino-based knockdown approach, we show functional contributions of Neurolin-a and Neurolin-b to distinct steps in RGC development. Neurolin-a is needed for a differentiation step that directly precedes axon outgrowth. In contrast, Neurolin-b is involved in RGC axon navigation between the chiasm and the optic tectum.

## MATERIALS AND METHODS

### Fish

Zebrafish were maintained at 28.5°C in the animal research facility of the University of Konstanz in compliance with animal welfare legislation. Embryos were collected after natural spawning, staged as previously described (Kimmel, 1989), and raised in egg water (0.3% w/v sea salt/0.0002% Methylene Blue) at 28.5°C. Transgenic zebrafish expressing membrane-targeted green fluorescent protein (GFP) under the control of the *brn3c* promoter in retinal axons (*tg(Brn3c:m-GFP)<sup>s56t</sup>*) were provided by H. Baier (University of California, San Francisco) and are described elsewhere (Xiao et al., 2005).

### Cloning and sequence analysis

Zebrafish and fugu *neurolin* genes and transcripts were identified by a combination of database searches, reverse transcription-polymerase chain reaction (RT-PCR), and 5'-rapid amplification of cDNA ends (RACE). Primer sequences and PCR conditions are available upon request, and cDNA sequences were deposited in GenBank (*Danio rerio neurolin-b*: DQ279080; *Takifugu rubripes neurolin-a*: DQ279082; *Takifugu rubripes neurolin-b*: DQ279081). Nucleotide sequences of tetrapod *neurolin* homologues were translated by using BioEdit (Hall, 1999) and aligned as aa by using ClustalW (Thompson et al., 1994). Phylogenies were reconstructed by using neighbor joining (NJ) methods with MEGA version 2.1 (Kumar et al., 2001), and support for nodes in the NJ tree was assessed by using 1,000 bootstrap reiterations (Felsenstein, 1985).

### Immunoblots

Anesthetized zebrafish embryos were homogenized in 2X protein sample buffer (312.5 mM Tris-Cl/10% sodium dodecyl sulfate [SDS]/50% glycerol/1% dithiothreitol [DTT], pH 6.8; 8  $\mu$ l per embryo). Ten microliters of homogenate were separated per lane on 8% SDS-polyacrylamide gels (Laemmli et al.,

1970) and transferred to Hybond C Super nitrocellulose membranes (GE Healthcare, Chalfont St. Giles, UK). After blocking with 3% milk powder/0.05% Tween 20/350 mM NaCl/phosphate-buffered saline (PBS); pH 7.4, primary anti-Neurolin mAb N287 (Leppert et al., 1999) was added. Immunoreactions were visualized with horseradish peroxidase (HRP)-coupled anti-mouse antibody and SuperSignal West Pico (Pierce, Rockford, IL).

### Morpholino injections

Morpholino (MO) antisense oligonucleotides (Summerton, 1999) were designed as follows by Gene Tools (Philomath, OR) to target *neurolin-a* and *neurolin-b* genes, respectively:

MO-Na: -33'-GTCCGGCGACAGTCTCAATAGAGAG'-57

MO-Nb: -7'-GCAGTCTGCGATAGTTCTGCACTCC'-31

MO oligonucleotides were diluted in 1X Danieau solution (58 mM NaCl/0.7 mM KCl/0.4 mM MgSO<sub>4</sub>/0.6 mM Ca(NO<sub>3</sub>)<sub>2</sub>/5 mM HEPES; pH, 7.6) to concentrations ranging from 1 to 3 mg/ml. Approximately 1.5 nl of MO or a buffer control solution (0.1% phenol red in 1X Danieau) was injected into the yolk of one- to two-cell-stage zebrafish embryos. To assess the specificity of the phenotype, a second morpholino targeting the 5'UTR of *neurolin-a* (MO-Na2; -15'-CCGGTTCTCCTTTATACA'-37; kindly provided by C.B. Chien) was injected and resulted in the same overall phenotype with reduced eye size and decreased RGC numbers. To exclude non-sequence-dependent activation of the p53 pathway, which can lead to cell death and morphological abnormalities, 2.5 ng of a morpholino targeting p53 (AGA-ATTGATTTGCCGACCTCCTCT) was injected together with MO-Na.

The efficiency of MO-Na in blocking Neurolin-a protein synthesis was assessed by Western blot analysis of embryo lysates at different stages of development (Supplementary Fig. 1). Because no antibody was available to detect Neurolin-b protein, a GFP-fusion construct was used to confirm that MO-Nb was capable of blocking translation of Neurolin-b (Supplementary Fig. 1).

### Determination of eye size

MO-Na and control buffer-injected embryos were fixed at 3 dpf and 6 dpf in 4% paraformaldehyde (PFA)/PBS. Eye diameter of wholemount embryos was determined under a dissecting microscope and set in relation to the torso length (nose to end of yolk ball).

### Histological sections

Embryos were fixed at 2 dpf and 4 dpf in 4% PFA/PBS and embedded in Durcupan (SPI Supplies, West Chester, PA). Sections (2–10  $\mu$ m) were made on a Reichert-Jung Autocut or a Reichert Om3 ultramicrotome and stained with Richardson's stain (1% Azuril/1% methylene blue/1% NaBH<sub>4</sub>). Due to the abnormal laterally and ventrally shifted position of the eyes in MO-Na-injected zebrafish (Fig. 4C), heads were cut obliquely, whereas frontal sections were cut for control fish. The number of cells in the retinal ganglion cell layer (RGCL) and inner nuclear layer (INL) were counted on single sections containing the optic nerve head. Apoptosis detection was performed on wholemount embryos, prior to sectioning, by using the ApoptTag<sup>®</sup> Peroxidase in situ Detection Kit (Qbiogene, Carlsbad, CA) following the manufacturer's instructions.

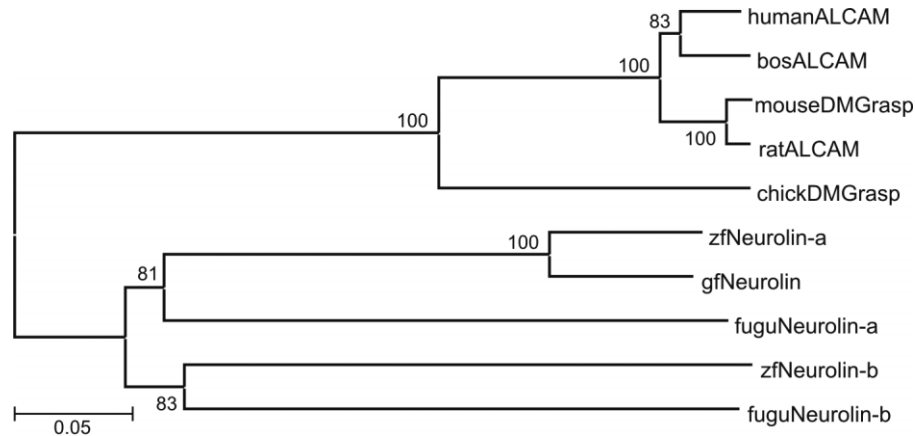


Figure 1. Phylogenetic relationship among vertebrate *neurolin* genes. The topology represents a consensus tree based on neighbor-joining (NJ) analysis of an amino acid (aa) alignment. Support for nodes is indicated (1,000 bootstrap reiterations). Scale represents 5% protein sequence divergence. chick, *Gallus gallus*; fugu, *Fugu rubripes*; gf, *Carassius auratus*; human, *Homo sapiens*; mouse, *Mus musculus*; rat, *Rattus norvegicus*; zf, *Danio rerio*.

### In situ hybridization and wholemount immunostaining

In situ hybridization and immunostaining were performed as previously described (Laessing and Stuermer, 1996; Ott et al., 2001). The following in situ probes were used: *neurolin-a* (bp 1,150–1,680 of NM\_131000; Laessing and Stuermer, 1996; Ott et al., 2001), *neurolin-b* (bp 1,125–1,632 of DQ279080), *atoh7* (bp 1–405 of NM\_131632; Masai et al., 2000), *shh* (bp 4–1,230 of NM\_131063.1; Kraus et al., 1993), and *irx1a* (bp 1–1,281 of NM\_207184.1; Cheng et al., 2006). The *pax2a* (NM\_131184; Krauss et al., 1991a) and *pax6* (X61389; Krauss et al., 1991b) in situ probes were kindly provided by S. Wilson.

The rabbit antiserum pAb 397 and the mouse monoclonal antibody mAb N518 recognizing Neurolin-a were prepared against native Neurolin protein immunopurified from adult goldfish brain membranes by using the original monoclonal antibody E21 (Ott et al., 1998, 2001). Both antibodies recognize a single band of ~85 kDa on Western blot and show identical staining patterns in the eye. Similarly, mAb T819 was produced by injecting purified recombinant zebrafish Tag1 protein into Balb/c mice. Hybridoma cell supernatants were screened for Tag1-specific staining on cryosections of goldfish and zebrafish brains as well as for the detection of a ~140 kDa single band in Western blots of fish central nervous system (CNS) tissue and recombinant Tag1 protein (Lang et al., 2001). The mAb E17 was generated by immunizing Balb/c mice with immunopurified goldfish E587 antigen (L1-like cell adhesion molecule). Specificity was tested on cryostat sections of the retina and optic tectum of adult goldfish and zebrafish, and a ~190 kDa band was detected on Western blot (Weiland et al., 1997). The mouse monoclonal antibodies mAb 5E11 for the detection of amacrine cells and their processes (Fadool et al., 1999) and mAb 1D1 for visualizing rod photoreceptors (Hyatt et al., 1996) were generated from splenocytes isolated from a Balb/c mouse immunized with whole zebrafish retina in Ribi adjuvant. Hybridoma supernatants were screened on frozen sections of adult retina and Western blots of total retinal protein and were kindly provided by P. Linser (Hyatt et al., 1996).

Confocal analysis of wholemount immunostaining was performed on a Zeiss LSM510 scanning confocal microscope. Figures were generated from stacks of 10–15 slices covering the thickness of the eye. Brightness and contrast were adjusted equally for each experiment performed by using CorelDRAW 12. Brightfield images were taken on a Zeiss Axioplan with brightness and contrast adjusted to highlight the in situ hybridization expression domains using CorelDRAW 12.

## RESULTS

### Expression analysis of the two zebrafish *neurolin* paralogs

By using a combination of Blast searches, RT-PCR, and RACE, we identified zebrafish *neurolin-b*, a paralog of *neurolin-a* (previously described by Kanki et al., 1994; Laessing et al., 1994). Searches in the fugu genome database also yielded two *neurolin* genes. Phylogenetic analysis of *neurolin* sequences resulted in a tree with distinct clades for the fish and the tetrapod genes, suggesting that *neurolin* duplicates (*neurolin-a* and *neurolin-b*) arose after the divergence of teleost and tetrapod lineages (Fig. 1). Calculation of nonsynonymous substitutions (aa) per nonsynonymous site (Nei and Gojobori, 1986) and separate comparison of each zebrafish *neurolin* gene to the human ortholog revealed comparable sequence distances (0.64 vs 0.66), indicating that both zebrafish duplicates evolved equally fast and are therefore equally related to human ALCAM. Overall, Neurolin-b protein is 48% identical to Neurolin-a and shares the same predicted structure of five extracellular Ig-like domains, a single transmembrane, and a short cytoplasmic domain, which showed the highest degree of conservation (75% identity).

To analyze whether Neurolin-a and Neurolin-b proteins might serve distinct or overlapping functions, the spatial distribution of Neurolin-b mRNA during zebrafish development was examined by wholemount in situ hybridization and compared with Neurolin-a (Kanki et al., 1994; Laessing and Stuermer, 1994; Fig. 2). During the preparation of this manuscript, a detailed analysis of Neurolin-b/Nlcam was published (Mann

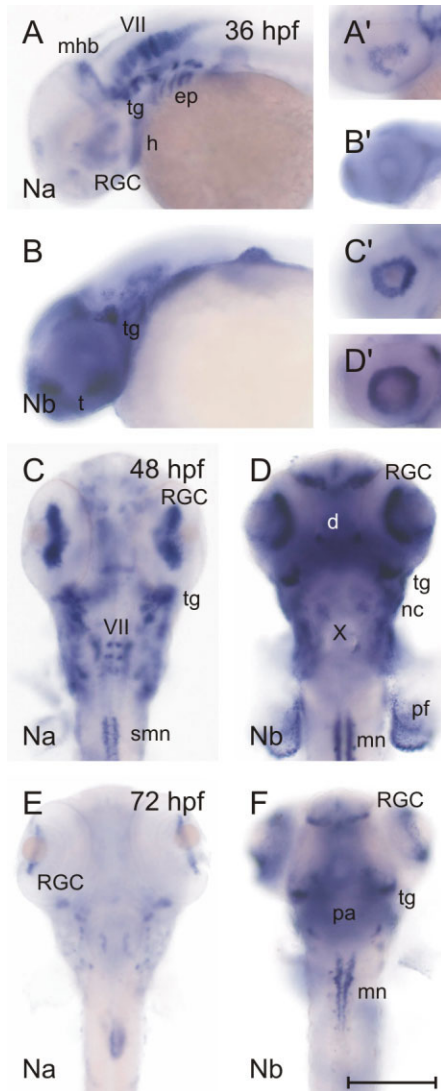


**Figure 2.** Comparative in situ hybridization analysis of zebrafish Neuroilin-a and Neuroilin-b expression. **A–D:** At 36 hpf (**A**) and 48 hpf (**C**), Neuroilin-a is found in RGCs, endodermal pouches (ep), heart (h), midbrain-hindbrain boundary (mhb), distinct cranial motor and sensory neurons (e.g., trigeminal ganglion [tg] facial nucleus [VII] and ganglion), and secondary motor neurons (smn) in the tail. Neuroilin-b (**B,D**) is detectable in the trigeminal ganglion (tg), telencephalon (t), diencephalon (d), neural crest cells (nc), vagus nucleus (X) and ganglion (out of focus), a band around the pectoral fins (pf), and motor neurons (mn) in the tail. **A',B':** In the retina, Neuroilin-a (**A'**) is seen in three quarters of the RGC layer at this stage. No Neuroilin-b mRNA (**B'**) was detectable in the eye at this stage. **C',D':** At 48 hpf, Neuroilin-a (**C'**) staining is found in RGCs all around the eye. Neuroilin-b (**D'**) transcripts are now also expressed in RGCs. **E,F:** With completion of neurogenesis and organogenesis ( $\geq 72$  hpf), Neuroilin-a (**E**) is drastically downregulated and only expressed in newly differentiating RGCs at the retinal margin. Level of Neuroilin-b expression (**F**) is clearly higher and particularly prominent in RGCs, the trigeminal ganglion (tg), and pharyngeal arches (pa). Control hybridizations with Neuroilin-a and Neuroilin-b sense probes yielded no signal at all embryonic stages analyzed (data not shown). Scale bar = 50  $\mu\text{m}$  in **F** (applies to **A–F**).

et al., 2006). In brief, Neuroilin-a and Neuroilin-b are expressed in distinct, but partially overlapping patterns. In the retina, where we analyzed the function of Neuroilin in detail, Neuroilin-a expression has been shown to be indicative of onset and progression of RGC differentiation. Accordingly, Neuroilin-a mRNA is seen in three-fourths of the RGC layer at 36 hpf (Fig. 2A,A') following the nasal over dorsal to temporal progressing differentiation wave (Laessing and Stuermer, 1996). At this stage, no Neuroilin-b mRNA was detectable in the eye (Fig. 2B,B'). Twelve hours later, the wave is completed (Fig. 2C,C'), by which time Neuroilin-a expression progresses in rings around the retinal margin and becomes confined to newborn RGCs (Fig. 2E). Neuroilin-b transcripts are found in RGCs at 48 hpf (Fig. 2D,D'), indicating a function later during retinal development. At 72 hpf, the Neuroilin-b expression domain resembles in principle the pattern of Neuroilin-a in RGCs but is broader (Fig. 2F). In summary, these overlapping but different spatiotemporal expression patterns of the zebrafish Neuroilin paralogs suggest a subfunctionalization of the duplicated genes.

### Knockdown of Neuroilin-a and Neuroilin-b leads to distinct morphological phenotypes

To examine the functions of the two Neuroilin paralogs during zebrafish development, we blocked translation of the respective mRNAs by using morpholino antisense oligonucleotides (MO) targeting either Neuroilin-a (MO-Na) or Neuroilin-b (MO-Nb) (Supplementary Fig. 1). MO-Na-treated zebrafish developed normally in the first 24 hours of development. Depending on the injected MO-Na dose, the mutant phenotypes ranged from moderate ( $\leq 1$  ng) to severe ( $\geq 5$  ng; Fig. 3C,D and data not shown) and became more pronounced with increasing age (data not shown). However, zebrafish injected even with high MO-Nb doses (7 ng, Fig. 3D) did not show any visible morphological changes during embryonic and larval development.

Overall, MO-Na-injected embryos seemed to develop slower and were smaller ( $\sim 10\%$ ) than their age-matched counterparts and died at about 6–8 dpf. They were less active but did respond vigorously to touch. Affected embryos exhibited an inflated heart cavity and deformed lower jaws (Fig. 3B,C). The eyes of MO-Na-injected embryos were slightly smaller than those of control larvae at 2 dpf (Fig. 3E,F). This difference was more pronounced at 3–6 dpf (Fig. 4A), and the eyes shifted into an abnormal ventromedial position at later stages of development (Fig. 3C and data not shown). This overall phenotype and in particular the small eyes was confirmed with a second independent morpholino (MO-Na2; see Materials and Methods) and by co-injection of a p53 morpholino (p53-MO: Supplementary Fig. 2). It has recently been shown that many morpholinos can sequence-independently activate the p53 pathway, leading to nonspecific small eye phenotypes. However, co-injection of p53-MO along with MO-Na did not change the observed phenotype, confirming that small eyes are caused by the specific suppression of Neuroilin-a expression (Supplementary Fig. 2).

At 3 dpf, MO-Na-injected embryos appeared darker than wild-type siblings, as they failed to adjust the distribution of melanin granules in their skin in bright light (Fig. 3G,H), suggesting that loss of Neuroilin-a function leads to blindness. Hence, further analysis was performed to investigate in detail the ocular phenotype of MO-Na- or MO-Nb-injected zebrafish and the functions of Neuroilin-a and Neuroilin-b with respect to the retina.

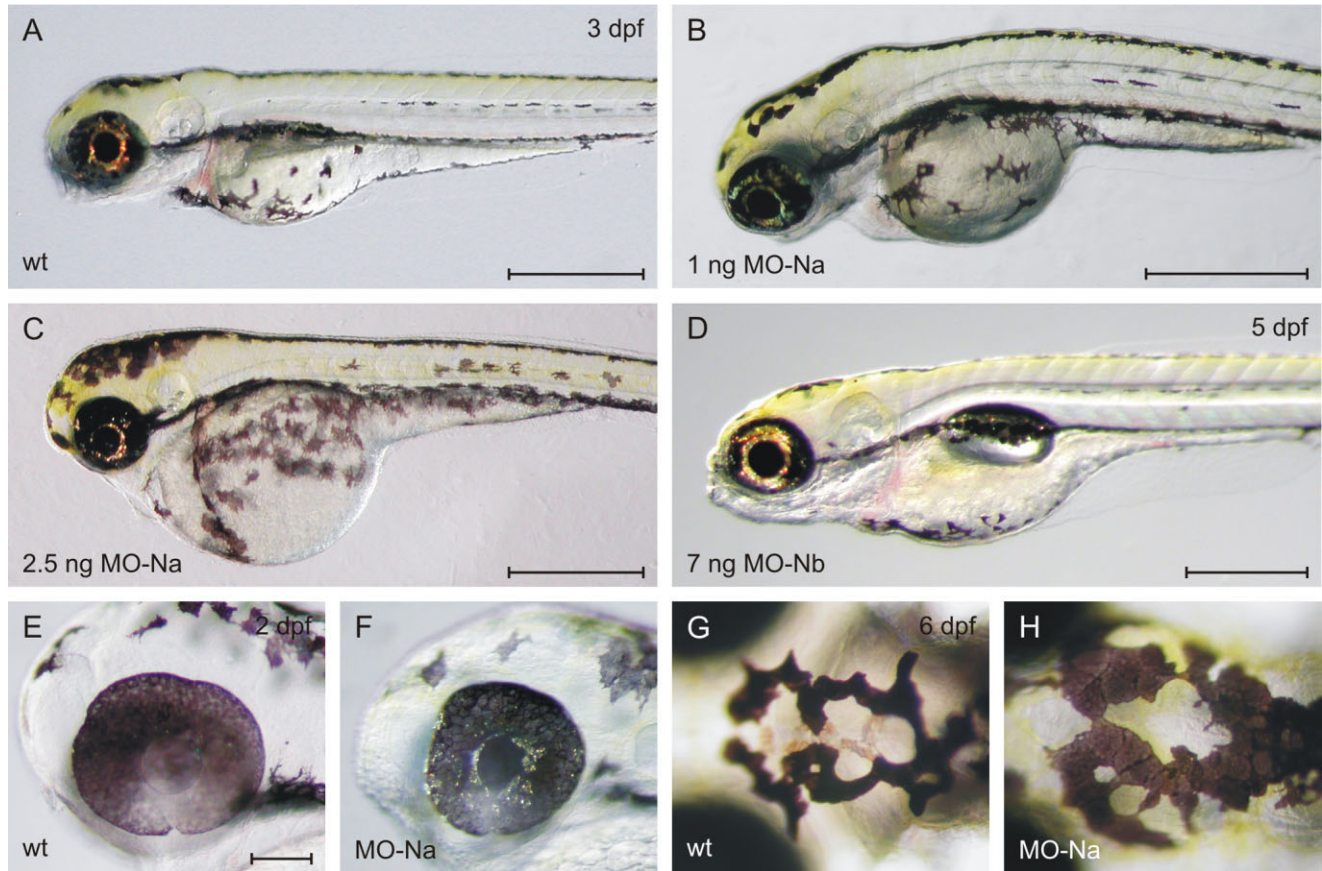


Figure 3.

Phenotypes of MO-N-injected zebrafish **A:** Wild-type control zebrafish at 3 dpf. **B,C:** Zebrafish injected either with 1 ng (**B**) or 2.5 ng (**C**) MO-Na. Concentration dependently, MO-Na-affected embryos are smaller and have an inflated heart cavity and reduced lower jaws. Their eyes are smaller and shifted into an abnormal ventromedial position. **D:** Zebrafish injected with 7 ng MO-Nb do not show visible morphological changes during development. **E,F:** Eye size of zebrafish injected with 2.5 ng MO-Na (**F**) is reduced in comparison with wild-type control embryos (**E**) as early as 2 dpf. **G,H:** In bright light conditions, melanin granules become contracted in wild-type embryos at 6 dpf (**G**). Larvae injected with 2.5 ng MO-Na (**H**) appear darker in the same conditions, because they fail to adjust the distribution of melanin in their skin, indicating that loss of Neuroilin-a function leads to blindness. **A-F:** Lateral views, anterior to the left. **G,H:** Dorsal views, anterior to the left. Scale bar = 500  $\mu\text{m}$  in **A-D**; 10  $\mu\text{m}$  in **E** (applies to **E, F**).

### Reduction of eye size and abnormal retina in MO-Na-injected zebrafish

The effect of loss of Neuroilin-a function on eye size was quantified by measuring the eye diameter of MO-Na-injected and age-matched buffer control-injected zebrafish (Fig. 4A). Because MO-Na fish are shorter than wild-type siblings (~10%) and showed abnormally bent tails at high MO concentrations, eye dimensions were set into relation to the respective torso length (head to end of yolk ball). Despite this correction, eye size was significantly reduced both in moderately (1 ng MO-Na) and severely (5 ng) affected embryos at 3 dpf. Smaller eyes were still obvious at 6 dpf, indicating that the defect could not be rescued at later stages of development when Neuroilin-a protein was re-expressed (Supplementary Fig. 1). To determine which cell type was affected in MO-Na-injected embryos, we counted cells within the RGCL and INL on transverse eye sections. Only approximately half the cells were present in both the RGCL and the INL in embryos injected with 2.5 ng MO-Na compared with wild-type

zebrafish (Fig. 4B). Therefore, the reduction in eye size is caused by the loss of RGCs and other neurons, implying that the whole retina is affected.

Morphological defects in the developing retina resulting from suppressed Neuroilin-a expression were analyzed in serial sections through the eyes of buffer-control and MO-Na-injected fish at 2 dpf and 4 dpf (Fig. 4C-F). The 2 dpf control retina (Fig. 4C) displayed differentiated RGCs and the beginning of RGC layer segregation from the INL (Nawrocki, 2002). Control larvae developed a distinct optic nerve head (ONH) through which RGC axons exit the retina. MO-Na counterparts, however, failed to exhibit a distinct RGC layer, and it is not clear whether RGCs had formed at all (Fig. 4D). The ONH was thin and seemed to consist only of glial cells (derivatives of early optic stalk cells; MacDonald et al., 1997). Along with an increase in retinal thickness, the segregation of the RGCL, INL, and photoreceptor layer (PRL) progressed in 4 dpf control retina (Fig. 4E). These sections exhibited more prominent ONHs and a zone of precursor cells at the retinal margin.

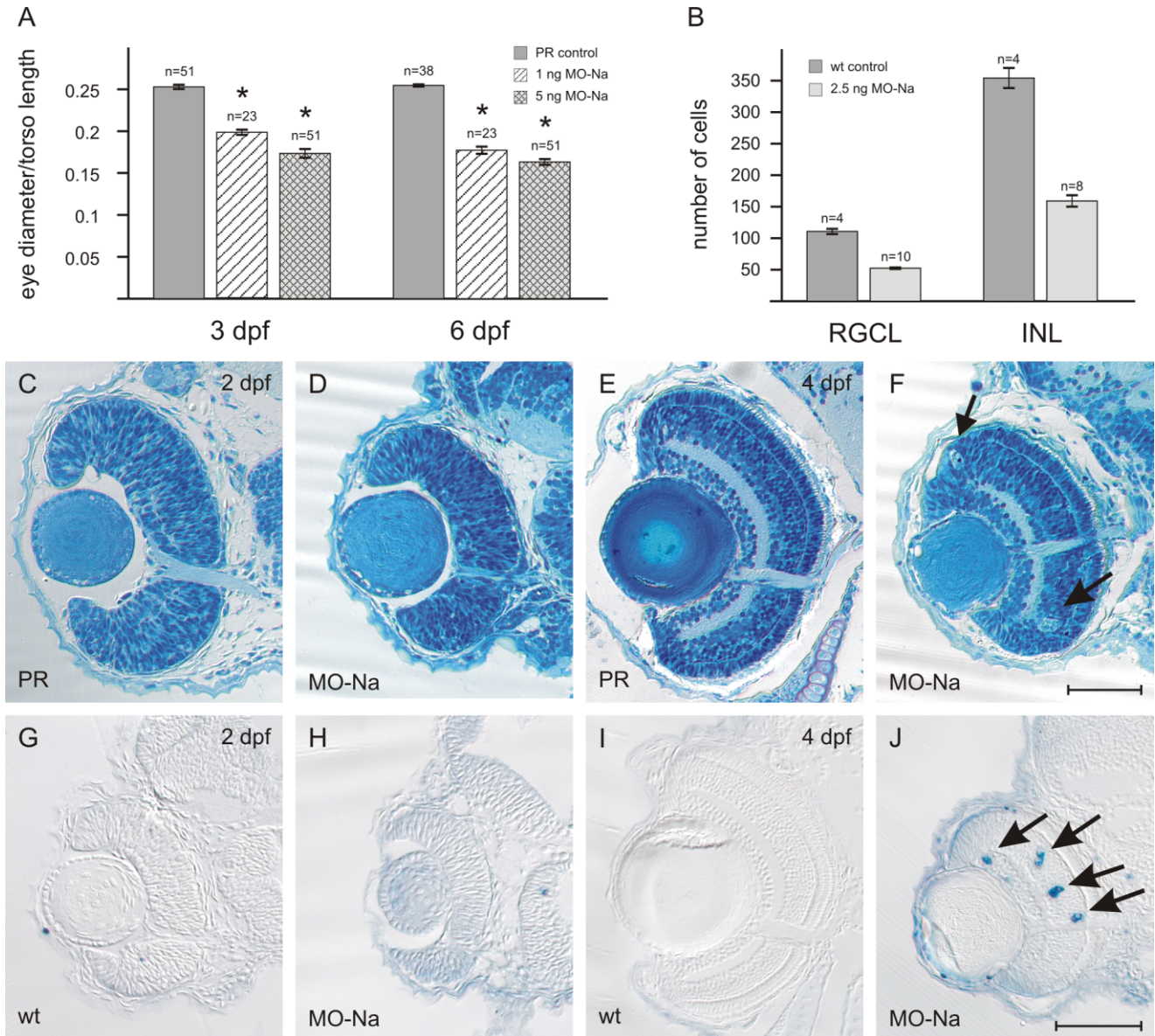


Figure 4.

Loss of Neurolin-a function leads to reduced eye size. **A**: Quantification of eye size in wholemount zebrafish injected either with 1 ng or 5 ng MO-Na in comparison with buffer control (PR) injected fish at 3 dpf and 6 dpf. Error bars are SD. **B**: Quantification of cells present in the retinal ganglion cell layer (RGCL) and the inner nuclear layer (INL) on eye sections of wild-type (wt) control and MO-Na-injected zebrafish at 4 dpf. Error bars are SD. **C–F**: Histological sections were stained with methylene blue to reveal retinal cell topology. Eyes of buffer-injected controls (PR) have differentiated RGCs and a distinct optic nerve (on) with axons at 2 dpf (C) and complete segregation of the retinal ganglion cell layer (RGCL), inner nuclear layer (INL), and photoreceptor layer (PRL) at 4 dpf (E). At 2 dpf, MO-Na counterparts are reduced in size and fail to exhibit a distinct RGC layer and the optic nerve head (onh) does not contain retinal axons (D). At 4 dpf, overall cell layering seems normal, but the onh is smaller (F). Note apoptotic nuclei in MO-Na eyes (arrows). \*, retinal marginal zone. **G–J**: Sections cut after detection of apoptotic cell death in wholemount embryos. No apoptotic cells are detected in wild-type eyes at 2 dpf (G) and 4 dpf (I) or in MO-Na eyes at 2 dpf (H). However, apoptosis is markedly increased in MO-Na-injected zebrafish at 4 dpf (J). Apoptotic cells are marked with arrows. **C–J**: left eyes, dorsal is to the top. Scale bar = 50  $\mu$ m in F (applies to C–F) and J (applies to G–J).

Although this order of retinal neurons was conserved in eyes of MO-Na-injected zebrafish (Fig. 4F), ONHs were either rudimentary or distinctly smaller compared with the control retina.

The presence of dark blue nuclei and cavities were striking feature of 4 dpf MO-Na retina (Fig. 4F), indicative of pyknotic or rather apoptotic cells (Cole and Ross, 2001; Neumann and Nüsslein-Volhard, 2000). By using TUNEL staining (Fig. 4G–J),

apoptotic cells were found to be rare in both wild-type and MO-Na-injected retina at 2 dpf (Fig. 4G,H; Biehlmaier et al., 2001). At 4 dpf, however, apoptosis was clearly increased in MO-Na compared with control retina (Fig. 4I,J). Stained nuclei occurred across the thickness of the retina, suggesting that retinal neurons in the RGCL, INL, and PRL undergo apoptosis at this later stage.

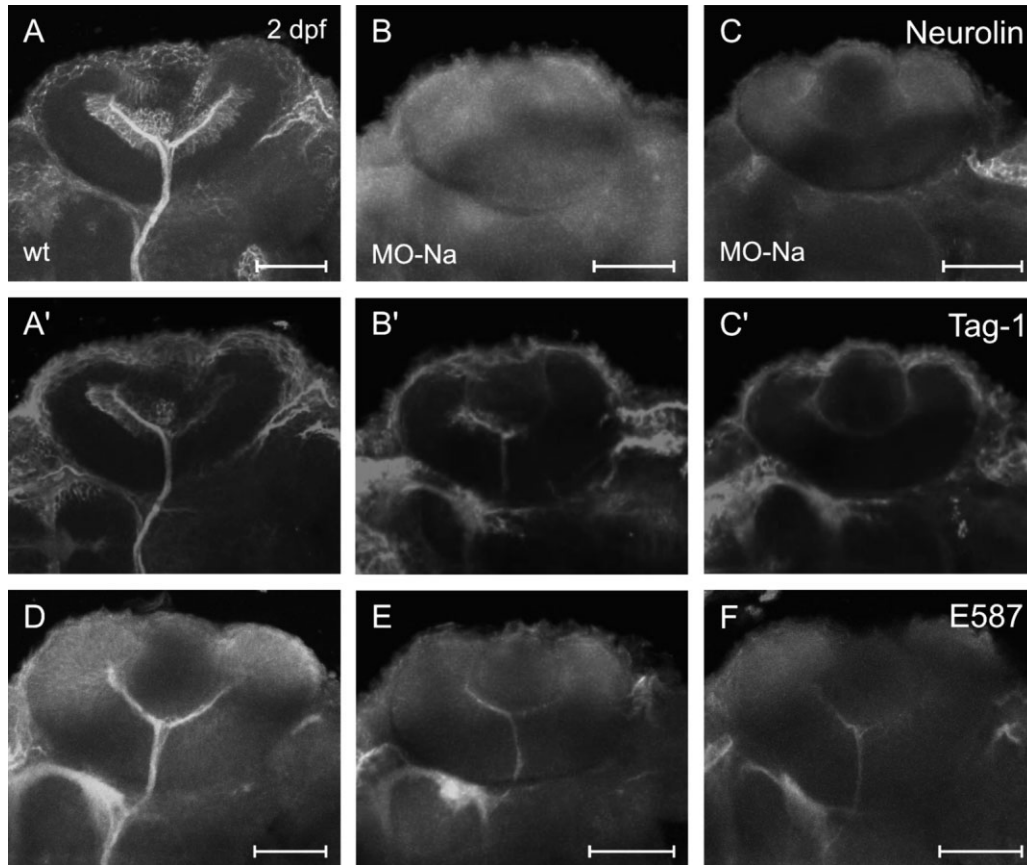


Figure 5.

Reduction of differentiated RGCs in MO-Na-injected zebrafish. Expression of markers indicative of differentiated RGCs was analyzed in zebrafish injected with 2.5 ng MO-Na (B,E: mild phenotype; C,F: severe phenotype) in comparison with wild-type (wt) controls (A,D). A–C: Double immunostaining with pAb $\alpha$ Neurolin (A–C) and mAb $\alpha$ Tag-1 (A'–C') antibodies showed no Neurolin protein in MO-Na-injected zebrafish (compare B,C with A) and reduced/no RGCs and axons (compare B',C' with A') at 2 dpf. D–F: mAb E587 immunostaining revealed only a thin optic nerve in MO-Na-injected embryos (E,F) compared with wt controls (D) at 2 dpf. A–F: dorsal views; anterior is to the left. Scale bar = 50  $\mu$ m in A–C (also applies to A'–C') and D–F.

### Loss of Neurolin-a function leads to arrest of RGC differentiation

In the retina, Neurolin-a is specifically expressed by differentiated RGCs and their axons (Laessing and Stuermer, 1996; this paper). To determine whether loss of Neurolin-a affects RGC development, we analyzed retinas of MO-Na-injected zebrafish with various retinal markers (Figs. 5, 6). Immunostaining using a polyclonal, Neurolin-a-recognizing antiserum confirmed expression of the protein on all RGCs and on retinal axons exiting the eye of wild-type siblings at 2 dpf (Fig. 5A). At this stage, no Neurolin-a was detected in either MO-Na- or MO-Na2-injected embryos (Fig. 5B,C; data not shown). Double-labeling with an  $\alpha$ Tag1 antibody, an IgSF protein expressed on RGCs and their axons (Fig. 5A'), revealed that only a few differentiated RGCs with a thin optic nerve (moderate phenotype; Fig. 5B') or no optic nerve (severe phenotype; Fig. 5C') were present in these retinas. Detection of the L1-like/E587 antigen (Weiland et al., 1997) expressed on retinal axons (Fig. 5D) gave similar results; only a few axons were seen in thin optic nerves in MO-Na-injected zebrafish (Fig. 5E,F).

To address whether these RGC defects in MO-Na morphants were caused by early patterning defects, we examined expres-

sion of *pax6* (early stage optic vesicle) and *pax2a* (midbrain-hindbrain boundary [MHB] and optic stalks). Expression patterns of both genes were comparable in MO-Na, MO-Nb, and control embryos at 24 hpf and 31 hpf (data not shown), indicating that neither Neurolin-a nor Neurolin-b were necessary for regionalization of the CNS or optic vesicle formation.

RGCs are the first retinal neurons to differentiate (Harris, 1997). Differentiation is initiated in a ventronasal cluster and then spreads fan-like to the temporal retina (Hu and Easter, 1999; Laessing and Stuermer, 1996). To determine whether this differentiation wave is impaired in MO-Na-injected zebrafish, we compared the distribution of Neurolin-a mRNA (Neurolin-a transcription is not impaired by MOs) in wild-type and experimental retina (Fig. 6A–D). Neurolin-a mRNA is normally expressed throughout the RGCL at 2dpf (Fig. 6A) and then becomes restricted to newly differentiated RGCs at the retinal margin (Fig. 6C). MO-Na-affected retina, however, showed Neurolin-a transcripts in only a few cells confined to a ventronasal cluster at both 2 dpf and 2.5 dpf (Fig. 6B,D), indicating that the wave of RGC differentiation was not only retarded but arrested due to the loss of Neurolin-a function. In contrast, expression of *ato7* mRNA, a bHLH transcription factor expressed prior to retinal neurogenesis and in-

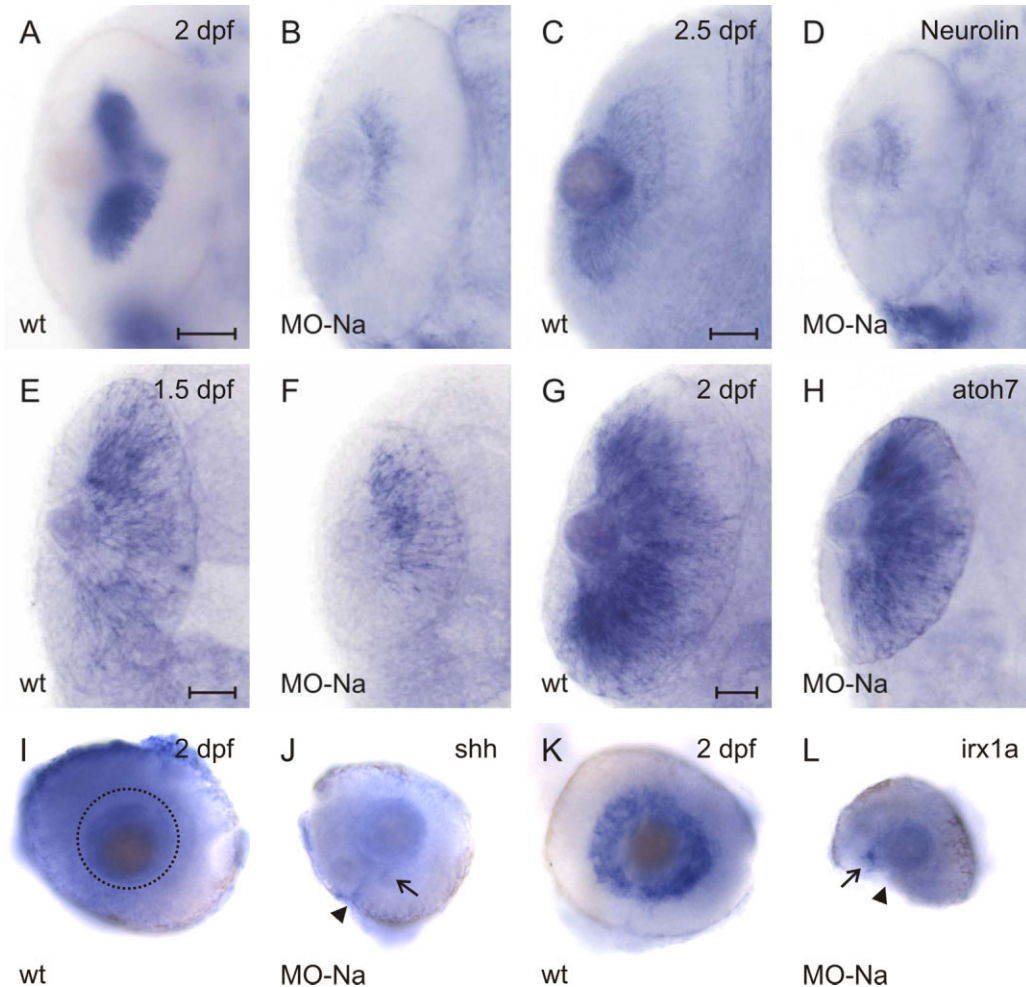


**Figure 6.** Arrested RGC differentiation in MO-Na-injected zebrafish. Expression of genes controlling RGC differentiation was analyzed by in situ hybridization in zebrafish injected with 2.5 ng MO-Na (B,D,F,H,J,L) in comparison with wild-type (wt) controls (A,C,E,G,I,K). **A–D:** Neurolin-a expression indicative of differentiated RGCs is detected throughout the whole retina in wt at 2 dpf (A) and becomes gradually restricted to the retinal margin at 2.5 dpf (C). In contrast, Neurolin-a mRNA is only detected in a small ventromedial cluster in MO-Na eyes at 2 dpf (B) and 2.5 dpf (D). **E–H:** Atoh7 mRNA levels are comparable in wt control (E,G) and MO-Na-injected (F,H) embryos at 1.5 dpf (E,F) and 2 dpf (G,H). **I,J:** Shh expression has spread around the retina in wt controls at 2 dpf (depicted by the circle, I) whereas shh mRNA could only be detected in a single cell in the ventronasal region in MO-Na eyes (arrow, J). The arrowhead marks the optic fissure. **K,L:** Expression of *irx1a* is found in only one to two RGCs in MO-Na eyes (arrow, L) in comparison with wt controls (K) at 2 dpf. The arrowhead marks the optic fissure. **A–H, K,L:** dorsal views; anterior is to the top. **I,J:** lateral views of dissected eyes. Scale bar = 50  $\mu$ m in A (applies to A,B), C (applies to C,D), E (applies to E,F), G (applies to G–L).

involved in specifying RGC cell fate (Masai et al., 2000; Kay et al., 2001), was only slightly retarded at 1.5 dpf (Fig. 6E,F) and was similar at 2 dpf (Fig. 6G,H) in MO-Na-injected compared with control retina, indicating that progenitor cells are nevertheless committed to the RGC fate. In contrast, markers of terminally differentiated RGCs like *shh* (Fig. 6I,J) and Iroquois homeobox gene *irx1a* (Fig. 6K,L) were only expressed in one to two cells in the ventronasal region in MO-Na retina compared with the ring-like expression in control fish at 2 dpf. Therefore, Neurolin-a function seems to be required for the terminal differentiation of RGCs.

### Impairment of RGC differentiation affects other retinal neurons

We next analyzed whether RGC differentiation is rescued at later stages of development and examined whether other

retinal neuron types are affected by impaired RGC development. For this purpose, we used transgenic zebrafish expressing membrane-targeted GFP in RGCs (Xiao et al., 2005) for MO injections, to allow simultaneous assessment of the formation of differentiated RGCs and their axons. GFP expression is slightly retarded with respect to RGC differentiation, but at 60 hpf (Fig. 7A) and especially at 72 hpf (Fig. 7E), GFP is detected in RGCs throughout the retina and in their axons projecting to the optic tectum. At both time points, either a few RGCs and a thin optic nerve (moderate phenotype; Fig. 7B,F) or no differentiated RGCs (severe phenotype; Fig. 7C,G) were visible in MO-Na-injected zebrafish. Analysis of MO-Nb fish revealed that RGC differentiation is generally slightly retarded in injected embryos (Fig. 7D), but RGCs are clearly present at 72 hpf (Fig. 7H), the time point for all further analysis. Counterstaining of transgenic fish with  $\alpha$ Tag1 antibody

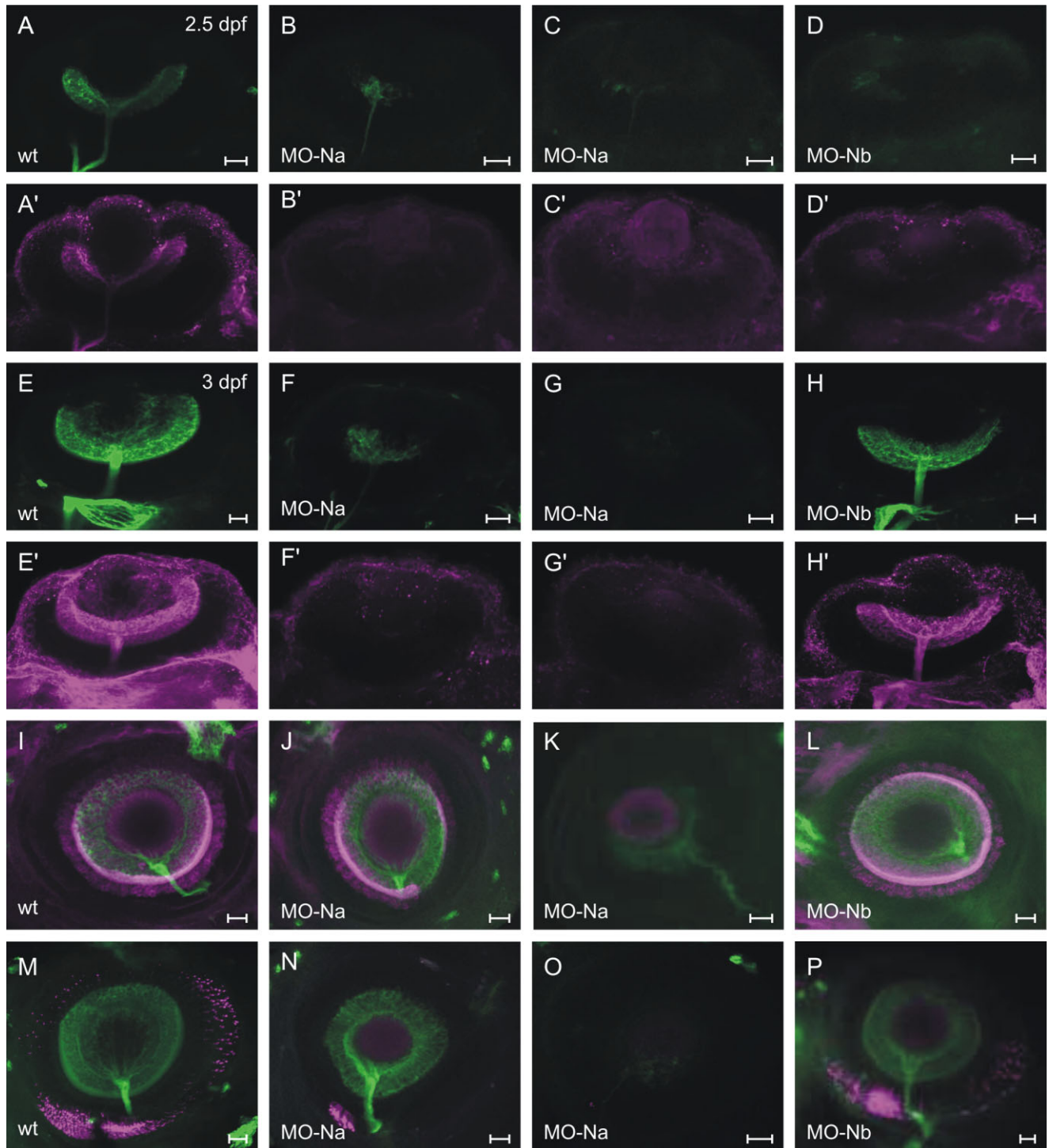


Figure 7.

Loss of Neuroilin-a, but not Neuroilin-b function affects differentiation of all retinal cell types. Transgenic zebrafish expressing GFP in RGCs (green, A–D, E–H, I–P) were used to assess the formation of differentiated RGCs and their axons in combination with antibody immunostaining to detect specific cell types. A–H: Immunostaining with mAb TAG-1 (A'–H') showed overlapping staining patterns with GFP expression (A–H), indicating that GFP fluorescence can be used to prove the existence of differentiated RGCs. At both 2.5 dpf (A–D) and 3 dpf (E–H), RGC differentiation is still impaired in embryos injected with 2.5 ng MO-Na (B,F: moderate phenotype; C,F: severe phenotype) compared with wild-type (wt) controls (A,E). Embryos injected with 5 ng MO-Nb showed slight retardation of RGC development at 2.5 dpf (compare D with A), but eyes are normal at 3 dpf (H). I–L: Development of amacrine cells (mAb 5E11, magenta) is either retarded (incomplete ring in moderate phenotype, J) or blocked (no magenta staining, severe phenotype, K) in MO-Na zebrafish in comparison with wt controls (full ring of amacrine cells, I) and MO-Nb-injected zebrafish (L) at 3 dpf. M–P: Differentiation of rod photoreceptors (mAb 1D1) is either delayed (small ventromedial cluster of magenta cells in moderate phenotype, N) or impaired (no magenta staining, severe phenotype, O) in MO-Na retina in comparison with wt controls (full ring of PR cells, M) and MO-Nb-injected zebrafish (P) at 3 dpf. A–H: dorsal views; anterior is to the left. I–P: lateral views; anterior is to the left. Scale bar = 20  $\mu\text{m}$  in A–D (also applies to A'–D'), E–H (also applies to E'–H'), I–P.

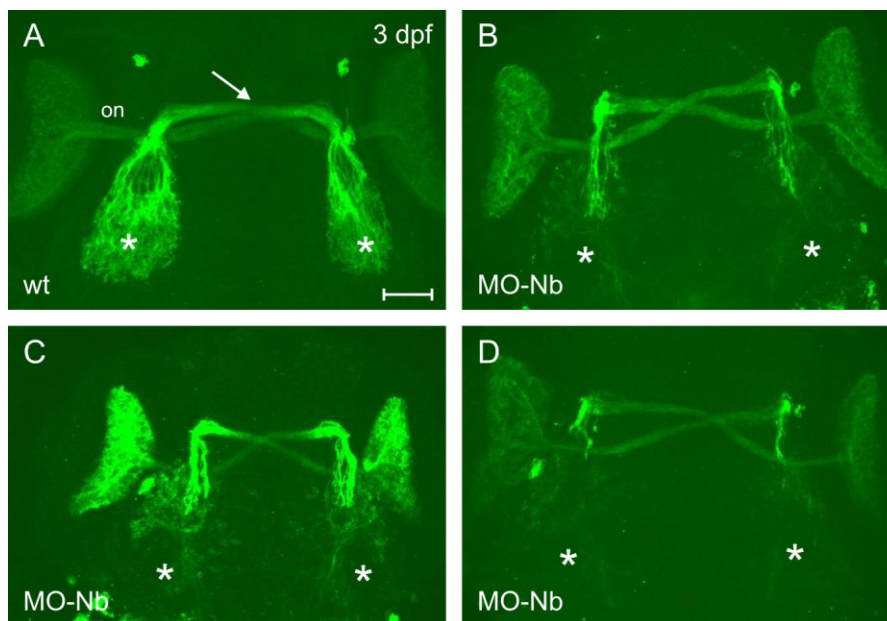


Figure 8.

Retinal axon pathfinding defects due to loss of Neurolin-b function. **A:** GFP-expressing RGC axons have grown along the optic nerve (on) and innervate the optic tectum (ot) at 3 dpf in wild-type (wt) control embryos. **B–D:** Injection of 5 ng MO-Nb causes aberrant pathfinding of RGC axons. Axons either fail to innervate the optic tectum (B), turn aberrantly within the tectal area (C), or do not find the optic tectum and stall prematurely (D). Arrow, optic chiasm; on, optic nerve; \*, optic tectum. Scale bar = 50  $\mu$ m in A (applies to A–D).

(Fig. 7A'–D', E'–H') showed that GFP expression nicely corresponded to the pattern of the RGC marker and that GFP detection is actually more sensitive because green fluorescence was sometimes seen in retina without  $\alpha$ Tag1 immunostaining (compare Fig. 7B,B' with F,F').

At 72 hpf, differentiation of amacrine cells in the INL was well established in wild-type control and MO-Nb-injected retina (Fig. 7I,L). In MO-Na zebrafish, the observed phenotype varied from almost normal slightly retarded if differentiated RGCs were present (Fig. 7J) to no detectable amacrine cells in fish with impaired RGC differentiation (Fig. 7K). At the same time, rod photoreceptor development had begun to spread across the retina in control and MO-Nb retina (Fig. 7M,P). In contrast, only a few photoreceptor cells confined to a ventro-nasal cluster (in eyes with differentiated RGCs and retinal axons) or no staining (eyes without differentiated RGCs) were detectable in retinas of MO-Na-injected zebrafish. Similar results were obtained with an antibody-detecting cone photoreceptors (data not shown). Therefore, development of other neuronal cells within the retina was also affected by the loss of Neurolin-a function and seemed to depend on the presence of differentiated RGCs. MO-Nb injection, in contrast, had no effect on the differentiation of retinal cells.

### Loss of Neurolin-b function is required late in retinotectal development

Injection of MO-Nb even at high concentrations did not produce an apparent phenotype by visual inspection (Fig. 3D) nor did it affect the timely differentiation of cell types in the retina (Fig. 7H',L,P). Expression of the retinal and brain markers *pax6*, *pax2a*, *shh*, and *irx1a* were also unchanged compared with controls at 31 hpf and 2 dpf (data not shown),

indicating a subtle function of Neurolin-b. Therefore, we decided to look for extraretinal axon defects in 3 dpf zebrafish. Analysis of GFP-labeled retinal axon on their path toward the optic tectum revealed striking abnormalities (Fig. 8A–D). In wild-type control embryos, retinal axons have reached the optic tectum and split into well-defined tracts prior to innervation of the dorsal and ventral tectal halves at 72 hpf (Fig. 8A; Stuermer, 1988). Growth of retinal axons into the optic nerve and up to the chiasm was normal in MO-Nb-injected zebrafish (Fig. 8B–D). However, severe pathfinding errors occurred once axons turned from the mediolateral to the anterior-posterior direction approaching the optic tectum. Axons either failed to split into the dorsal and ventral tracts to innervate their target (7/15 samples; Fig. 8B), turned aberrantly within the tectal field (6/15 samples; Fig. 8C), or did not find the optic tectum and prematurely stopped (2/15 samples; Fig. 8D). Clearly, unlike Neurolin-a, Neurolin-b is not involved in RGC differentiation but is necessary for correct RGC axon projection and innervation of the optic tectum.

## DISCUSSION

RGC differentiation is governed by a cascade of gene activation controlling the sequence of distinct developmental stages and promoting axon growth and navigation. By using translation-blocking MOs targeting either of the two Neurolin paralogs, Neurolin-a or Neurolin-b, our study shows that the two gene products have specialized their function because of duplication and each plays a crucial, but distinct role in RGC development. Neurolin-a is necessary for a step in the differentiation of RGCs that correlates with axogenesis (Stuermer, 1988; Laessing and Suermer, 1996). Loss of Neurolin-a ex-

pression inhibits the timely differentiation of RGCs and non-RGC neurons and ultimately leads to cell death. The resulting abnormal retinas lack axons and optic nerves and are probably nonfunctional. Neuroilin-b expression in RGCs is delayed relative to Neuroilin-a, but is present during axon growth and navigation toward the optic tectum. Accordingly, loss of Neuroilin-b expression does not impair RGC differentiation, and eyes develop normally. However, the absence of Neuroilin-b causes strikingly aberrant pathways of RGC axons and failure to correctly invade the optic tectum. Together, our results show novel functions of Neuroilin/ALCAM in the development of the retina and the formation of tectal connections.

### Importance of Neuroilin-a during RGC differentiation

In our earlier work, we identified the dynamic spatiotemporal sequence of RGC differentiation in zebrafish by the expression of Neuroilin-a (Laessing and Stuermer, 1996). Expression proceeds in an arc-like pattern from the nasal via dorsal to temporal and ventral retina and then continues in rings in progressively more peripheral positions (Laessing and Stuermer, 1996). In our present experiments, inhibition of Neuroilin-a protein synthesis disrupted this pattern of RGC differentiation and blocked the normal order of retina growth, causing reduced eye size. These results suggest that Neuroilin-a-based cell-cell communication is necessary for the progression of cell differentiation across the retina. A challenge for future experiments is the analysis of the intracellular signaling cascades triggered by these interactions.

Several other genes involved in zebrafish retinal development are similarly expressed in a wave-like pattern. Both *shh* and the Iroquois homeobox gene *irx1a* are required for the propagation of the RGC differentiation wave across the retina (Neumann and Nüsslein-Volhardt, 2000; Cheng et al., 2006). Sonic you (*syu*) mutant zebrafish as well as *irx1a* morphants show retinal defects that closely resemble MO-Na-affected retinæ. Eyes are smaller and development of RGCs is impaired as the spreading waves of *shh/irx1a* expression are collapsed (Neumann and Nüsslein-Volhardt, 2000; Stenkamp et al., 2002; Cheng et al., 2006). Whether this similar phenotype implies any interactions among *irx1a*, *shh*, and Neuroilin signaling pathways remains to be analyzed. Interestingly, absence of either *shh*, *irx1a*, or Neuroilin-a also leads to impaired differentiation of neurons in the INL and PRL. It has been shown that *shh*, secreted by amacrine cells, acts as a short-range signal to direct differentiation and lamination in the absence of RGCs (Shkumatava et al., 2004). Therefore, loss of all *shh* sources explains the retinal phenotype of *syu* mutants. *Ir1a* and Neuroilin-a, however, are expressed only on RGCs (Laessing and Stuermer, 1996; Leppert et al., 1999; Cheng et al., 2006). Although others have claimed Neuroilin-a expression in the early eye anlage (Mann et al., 2007) and in amacrine cells (Kay et al., 2001), we and others could not find this by either *in situ* hybridization or immunostaining (Laessing and Stuermer, 1999; Shkumatava et al., 2004; this paper). RGCs are generally the first retinal neurons to differentiate, and it has been shown that they affect the subsequent differentiation of neurons in a cohort that derives from a common progenitor cell (Harris, 1997).

The bHLH transcription factor *atoh7* is induced in the first RGCs by *pax2a*-expressing optic stalk cells in the nasoventral retina prior to Neuroilin-a and participates in the induction of

RGC cell fate (Masai et al., 2000; Kay et al., 2001). The progression of this induction wave is independent of differentiated RGCs (Kay et al., 2005). An early role for *atoh7* in RGC cell fate priming upstream of Neuroilin-a function is consistent with our results showing that the wave of *atoh7* expression is unaltered in MO-Na-injected zebrafish embryos. Therefore, *atoh7* expression is necessary but not sufficient for retinal progenitors to develop into RGCs. Because the optic cup (*pax6* expression) and optic stalk (*pax2a* expression) are normal in MO-Na-treated zebrafish, Neuroilin-a functions in RGC differentiation after cell fate determination by *atoh7*. Surprisingly, an early cell fate error, such as that seen in the *atoh7* null mutant *lakritz* (*lak*; Kay et al., 2001), seems less detrimental to retinal development than later block of RGC differentiation such as that observed in *shh* mutants and *irx1a* and Neuroilin-a MO knockdowns (Neumann and Nüsslein-Volhardt, 2000; Stenkamp et al., 2002; Cheng et al., 2006; this paper). Although no RGCs differentiate in *lak*, all other retinal cells develop normally in organized lamina. Rather than losing cells, *lak* mutants overproduce bipolar, amacrine, and Müller glia cells and misplaced amacrine cells populate the prospective RGCL. Because progenitor cells are not restricted to the RGC fate by *atoh7* expression in *lak*, they can “switch” to a different cell type. The multipotent progenitor cells change their competence to generate different retinal cells in response to tightly controlled position- and stage-dependent environmental cues (Livesey and Cepko, 2001).

Analysis of the zebrafish mutant ascending and descending (*add*) gene revealed that histone deacetylase 1 (*hdac1*) regulates cell cycle exit as the first step of retinal neurogenesis by suppressing Wnt and Notch signaling pathways (Yamaguchi et al., 2005). Division of retinal progenitors produces two daughters, one of which becomes a postmitotic RGC (Poggi et al., 2005). Based on the *atoh7*, *shh*, *irx1a*, and Neuroilin-a knockdown phenotypes, we propose a model in which cells committed to the RGC fate due to *atoh7* expression would produce a signaling molecule that would inhibit adjacent progenitor cells to differentiate. Because the differentiation of the different retinal cells is temporally controlled (Ohnuma et al., 2002), this would prevent all progenitor cells from becoming RGCs. One candidate signaling molecule is Notch, which has been shown to maintain proliferation and to inhibit differentiation (Yamaguchi et al., 2005). Once the cells committed to the RGC cell fate actually develop into differentiated RGCs, and hence express *shh*, *irx1a*, and Neuroilin-a, they then start to express a de-repressor (for example, *shh* itself) to lift the inhibition of differentiation and to allow progenitors to develop into other cell types like amacrine or photoreceptors.

In accordance with this inhibitor/de-repressor model, loss of *atoh7* expression would result in the loss of the differentiation inhibitor, and progenitor cells would be free to develop into all cells except RGCs (*lak* phenotype). Loss of Neuroilin-a (and *irx1a*), however, would mean persistent block of differentiation of all cell types because the inhibitor cannot be de-repressed, as observed in *irx1a* and Neuroilin-a morphant phenotypes. Because this inhibition/de-repression has to occur very dynamically and be spatiotemporally controlled, it will be challenging to analyze without knowledge of the molecules involved. It would be interesting to know whether Notch expression is at all altered in *lak/atoh7* mutants.

Another feature of MO-Na-affected eyes is the presence of fragmented nuclei and cavities indicative of neuronal apoptosis. Again, these are not restricted to the RGCL but are found in all retinal layers and are only detected at later stages of retinal development (4 dpf) well after onset of Neuroilin-a expression (32 hpf) and the appearance of a MO-Na phenotype. In *syu* mutant and *irx1a* morphant retinas, apoptosis also occurs late and spatially random (Neumann and Nüsslein-Volhardt, 2000; Stenkamp et al., 2002; Cheng et al., 2006). Cells that have left the cycle but are not able to complete their differentiation program within a certain time period seem to be condemned to die.

### Involvement of Neuroilin-b in RGC axon pathfinding

Loss of Neuroilin-b function did not produce an overall morphological phenotype. Because Neuroilin-b was found to be expressed late ( $\geq 48$  hpf) in differentiated RGCs, differentiation of retinal cells is unaffected by loss of Neuroilin-b function. Instead, Neuroilin-b has a role during axon growth and innervation of the optic tectum. In wild-type zebrafish, the first RGC axons enter the tectum at 48 hpf and reach its posterior end within the next 24 hpf (Stuermer, 1988). In MO-Nb-injected zebrafish, retinal axons defasciculate in the region between the left and right eye after crossing at the chiasm and stall at the anterior end of the optic tectum or grow to abnormal positions. Therefore, late expression of Neuroilin-b in RGCs in comparison with Neuroilin-a correlates with a late function in the developing visual system. The observed phenotype suggests a role for Neuroilin-b in RGC axon pathfinding and fasciculation not within the retina (Ott et al., 1998; Leppert et al., 1999) but toward the optic tectum.

In the goldfish retina, Neuroilin is involved in intraretinal axon pathfinding as the radial growth of axons from newborn RGCs becomes highly abnormal and defasciculated in the presence of Neuroilin antibodies (Ott et al., 1997; Leppert et al., 1999). We have not analyzed the pathways of axons within the zebrafish retina of 48 hpf zebrafish because, in our hands, these are too small for such investigations. The avian homologue DM-GRASP has also been associated with axon growth and the establishment of neural connections (Burns et al., 1991; Pourquie et al., 1992; Pollerberg and Mack, 1994; DeBernardo and Chang, 1996). In the presence of DM-GRASP F(ab) fragments, axons fail to enter the optic nerve and stray away from correctly orientated axons (Avci et al., 2004). Similarly, ALCAM knockout mice show fasciculation and pathfinding defects of RGC and motoraxons (Weiner et al., 2004). The ALCAM knockout retina is normally stratified, but axons fascicles in the optic fiber layer are broader, and aberrant trajectories are observed. Consequently, an axon guidance function, either within the retina (goldfish) or the trajectory to the tectum (mice, zebrafish) seems to be evolutionarily conserved for the *neuroilin/alcam* gene.

In addition to the axon fasciculation and pathfinding defects, the ALCAM knockout retina shows retinal dysplasia indicative of aberrant growth and development. Although this defect was not analyzed in temporal detail or with differentiation markers to elucidate which phase of retinal development was affected, mouse ALCAM also seems to have a basic role in cell differentiation similar to Neuroilin-a in zebrafish. However, as mouse ALCAM is still present on neonatal and adult retinal axons (Weiner et al., 2004), it cannot provide a dynamic function that has to be timely and spatially controlled, as is

Neuroilin-a, which is only expressed in newborn retinal ganglion cells and is downregulated a few hours later (Laessing and Stuermer, 1996). Neuroilin-a function in the regulation of cell type specification seems therefore to be specific to zebrafish, which would also explain how RGCs properly differentiate and send axons out of the eye in the ALCAM knockout mouse. In contrast, human ALCAM is important for the differentiation of various cell types (hematopoieses: Cortes et al., 1999; Uchida et al., 1997; Ohneda et al., 2001; thymus development: Bowen et al., 1995; bone morphogenesis: Bruder et al., 1998).

Our present data demonstrate that cell differentiation, namely, of retinal cells but also of red blood cells (unpublished result), and axon pathfinding are mediated by two proteins in zebrafish, Neuroilin-a and Neuroilin-b, respectively. This is in agreement with the duplication-degeneration-complementation (DDC) model that proposes a partitioning of gene functions following gene duplication that renders both duplicates necessary to preserve the function of the single ancestral gene (Force et al., 1999; Meyer and Schartl, 1999).

### ACKNOWLEDGMENTS

We thank H. Baier (University of California) for provision of transgenic *brn3c:GFP* zebrafish, M. Klinger for help with injections, S. Hannbeck for technical assistance, and A.Y. Loos for zebrafish care.

### LITERATURE CITED

- Avci HX, Zelina P, Thelen K, Pollerberg GE. 2004. Role of the cell adhesion molecule DM-GRASP in growth and orientation of retinal ganglion cell axons. *Dev Biol* 271:291–305.
- Bastmeyer M, Leppert CA, Ott H, Stuermer CAO. 1995. Fish E587 glycoprotein, a member of the L1 family of cell adhesion molecules, participates in axonal fasciculation and the age-related order of ganglion cell axons in the goldfish retina. *J Cell Biol* 130:969–976.
- Biehlmaier O, Neuhauss SCF, Kohler, K. 2001. Onset and time course of apoptosis in the developing zebrafish retina. *Cell Tissue Res* 306:199–207.
- Cepko CL. 1999. The roles of intrinsic and extrinsic cues and bHLH genes in the determination of retinal cell fates. *Curr Opin Neurobiol* 9:37–46.
- Cheng CW, Yan CHM, Hui C, Strahle U, Cheng S H. 2006. The homeobox gene *irx1a* is required for the propagation of the neurogenic waves in the zebrafish retina. *Mech Dev* 123:252–263.
- Cole LK, Ross LS. 2001. Apoptosis in the developing zebrafish embryo. *Dev Biol* 240:123–142.
- Cortes F, Deschaseaux F, Uchida N, Labastie MC, Frieria AM, He D, Charbord P, Peault B. 1999. HCA, an immunoglobulin-like adhesion molecule present on the earliest human hematopoietic precursor cells, is also expressed by stromal cells in blood-forming tissues. *Blood* 93:826–837.
- DeBernardo AP, Chang S. 1996. Heterophilic interactions of DM-GRASP: GRASP-NgCAM interactions involved in neurite extension. *J Cell Biol* 133:657–666.
- Deiner MS, Kennedy TE, Fazeli A, Serafini T, Tessier-Lavigne M, Sretavan DW. 1997. Netrin-1 and DCC mediate axon guidance locally at the optic disc: loss of function leads to optic nerve hypoplasia. *Neuron* 19:575–589.
- Dickson BJ. 2002. Molecular mechanisms of axon guidance. *Science* 298:1959–1964.
- Dingwell KS, Holt CE, Harris WA. 2000. The multiple decisions made by growth cones of RGCs as they navigate from the retina to the tectum in *Xenopus* embryos. *J Neurobiol* 44:246–259.
- Fadool JM, Fadool DA, Moore JC, Linser PJ. 1999. Characterization of monoclonal antibodies against zebrafish retina. *Invest Ophthalmol Visual Sci Suppl* 40:1251.
- Fashena D, Westerfield M. 1999. Secondary motoneuron axons localize DM-GRASP on their fasciculated segments. *J Comp Neurol* 406:415–424.
- Felsenstein J. 1985. Confidence limits on phylogenies: an approach using the bootstrap. *Evolution* 39:783–791.

- Hall TA. 1999. BioEdit: a user-friendly biological sequence alignment editor and analysis program for Windows 95/98/NT. *Nucleic Acids Symp Ser* 41:95–98.
- Harris WA. 1997. Cellular diversification in the vertebrate retina. *Curr Opin Genet Dev* 7:651–658.
- Hu M, Easter SS. 1999. Retinal neurogenesis: the formation of the initial central patch of postmitotic cells. *Dev Biol* 207:309–321.
- Hyatt GA, Schmitt EA, Fadool JM, Dowling JE. 1996. Retinoic acid alters photoreceptor development in vivo. *Proc Natl Acad Sci U S A* 93:13298–13303.
- Kanki JP, Chang S, Kuwada JY. 1994. The molecular cloning and characterization of potential chick DM-GRASP homologs in zebrafish and mouse. *J Neurobiol* 25:831–845.
- Kay JN, Finger-Baier KC, Roeser T, Staub W, Baier H. 2001. Retinal ganglion cell genesis requires lakritz, a zebrafish atonal homolog. *Neuron* 30:725–736.
- Kay JN, Link BA, Baier H. 2005. Staggered cell-intrinsic timing of atoh7 expression underlies the wave of ganglion cell neurogenesis in the zebrafish retina. *Development* 132:2573–2585.
- Kimmel CB. 1989. Genetics and early development of zebrafish. *Trends Genet* 5:283–288.
- Klinger M, Taylor JS, Oertle T, Schwab ME, Stuermer CA, Diekmann H. 2004. Identification of Nogo-66 receptor (NgR) and homologous genes in fish. *Mol Biol Evol* 21:76–85.
- Krauss S, Johansen T, Korzh V, Moens U, Ericson JU, Fjose A. 1991a. Zebrafish pax[zf-a]: a paired box-containing gene expressed in the neural tube. *EMBO J* 10:3609–3619.
- Krauss S, Johansen T, Korzh V, Fjose A. 1991b. Expression of the zebrafish paired box gene pax[zf-b] during early neurogenesis. *Development* 113:1193–1206.
- Krauss S, Concordet J P, Ingham PW. 1993. A functionally conserved homolog of the *Drosophila* segment polarity gene hh is expressed in tissues with polarizing activity in zebrafish embryos. *Cell* 75:1431–1444.
- Kumar S, Tamura K, Jakobsen IB, Nei M. 2001. MEGA2: Molecular Evolutionary Genetics Analysis software. Tempe, Arizona.
- Laemmli UK, Beguin, F, Gujer-Kellenberger, G. 1970. A factor preventing the major head protein of bacteriophage T4 from random aggregation. *J Mol Biol* 47:69–85.
- Laessing U, Stuermer CAO. 1996. Spatiotemporal pattern of retinal ganglion cell differentiation revealed by the expression of neurodin in embryonic zebrafish. *J Neurobiol* 29:65–74.
- Laessing U, Giordano S, Lottspeich F, Stuermer CAO. 1994. Molecular characterization of fish neurodin: a growth associated cell surface protein and member of the immunoglobulin superfamily in the fish retinotectal system with similarities to chick protein DM-GRASP/SC-1/BEN. *Differentiation* 56:21–29.
- Lang DM, Warren JT Jr, Klisa C, Stuermer CAO. 2001. Topographic restriction of TAG-1 expression in the developing retinotectal pathway and target dependent reexpression during axon regeneration. *Mol Cell Neurosci* 17:398–414.
- Leppert CA, Diekmann H, Paul C, Laessing U, Marx M, Bastmeyer M, Stuermer CAO. 1999. Neurodin Ig domain 2 participates in retinal axon guidance and Ig domains 1 and 3 in fasciculation. *J Cell Biol* 144:339–349.
- Livesey FJ, Cepko CL. 2001. Vertebrate neural cell-fate determination: lessons from the retina. *Nat Rev Neurosci* 2:109–118.
- MacDonald R, Scholes J, Straehle U, Brennan C, Holder N, Brand M, Wilson SW. 1997. The Pax protein Noi is required for commissural axon pathway formation in the rostral forebrain. *Development* 124:2397–2408.
- Mann CJ, Hinitz Y, Hughes S M. 2006. Comparison of neurodin (ALCAM) and neurodin-like cell adhesion molecule (NLCAM) expression in zebrafish. *GEP* 6:952–963.
- Masai I, Stemple DL, Okamoto H, Wilson SW. 2000. Midline signals regulate retinal neurogenesis in zebrafish. *Neuron* 27:251–263.
- Meyer A, Scharl M. 1999. Gene and genome duplications in vertebrates: the one-to-four (-to-eight in fish) rule and the evolution of novel gene functions. *Curr Opin Cell Biol* 11:699–704.
- Nawrocki W. 2002. Development of the neural retina in the zebrafish, *Brachydanio rerio*. PhD thesis, University of Oregon, Eugene, OR.
- Nei M, Gojobori T. 1986. Simple methods for estimating the numbers of synonymous and nonsynonymous nucleotide substitutions. *Mol Biol Evol* 3:418–426.
- Neumann CJ, Nüsslein-Volhard C. 2000. Patterning of the zebrafish retina by a wave of sonic hedgehog activity. *Science* 289:2137–2139.
- Ohneda O, Ohneda K, Arai F, Lee J, Miyamoto T, Fukushima Y, Dowbenko D. 2001. ALCAM (CD166): its role in hematopoietic and endothelial development. *Blood* 98:2134–2142.
- Ohno S. 1999. Gene duplication and the uniqueness of vertebrate genomes circa 1970–1999. *Semin. Cell Dev Biol* 10:517–522.
- Ohnuma S, Hopper S, Wang KC, Philpott A, Harris WA. 2002. Co-ordinating retinal histogenesis: early cell cycle exit enhances early cell fate determination in the *Xenopus* retina. *Development* 129:2435–2446.
- Ott H, Bastmeyer M, Stuermer CAO. 1998. Neurodin, the goldfish homolog of DM-GRASP, is involved in retinal axon pathfinding to the optic disk. *J Neurosci* 18:3363–3372.
- Ott H, Diekmann H, Stuermer CAO, Bastmeyer M. 2001. Function of neurodin (DM-GRASP/SC-1) in guidance of motor axons in zebrafish embryos. *Dev Biol* 235:86–97.
- Paschke KA, Lottspeich F, Stuermer CAO. 1992. Neurodin, a cell surface glycoprotein on growing retinal axons in the goldfish visual system, is reexpressed during retinal axonal regeneration. *J Cell Biol* 117:863–875.
- Poggi L, Vitorino M, Masai I, Harris WA. 2005. Influences on neuronal lineage and mode of division in the zebrafish retina in vivo. *J Cell Biol* 171:991–999.
- Pollerberg GE, Mack TG. 1994. Cell adhesion molecule SC1/DMGRASP is expressed on growing axons of retina ganglion cells and is involved in mediating their extension on axons. *Dev Biol* 165:670–687.
- Pourquie O, Corbel C, Le Caer JP, Rossier J, Le Douarin NM. 1992. BEN, a surface glycoprotein of the immunoglobulin superfamily, is expressed in a variety of developing systems. *Proc Natl Acad Sci USA* 89:5261–5265.
- Robu ME, Larson JD, Nasevicius A, Beiraghi S, Brenner C, Farber SA, Ekker SC. 2007. p53 activation by knockdown technologies. *PLoS Genet* 3:788–801.
- Rougon G, Hobert O. 2003. New insights into the diversity and function of neuronal immunoglobulin superfamily molecules. *Annu Rev Neurosci* 26:207–238.
- Shkumatava A, Fischer S, Muller F, Strahle U, Neumann CJ. 2004. Sonic hedgehog, secreted by amacrine cells, acts as a short-range signal to direct differentiation and lamination in the zebrafish retina. *Development* 131:3849–3858.
- Stenkamp DL, Frey RA, Mallory DE, Shupe EE. 2002. Embryonic retinal gene expression in sonic-you mutant zebrafish. *Dev Dyn* 225:344–350.
- Stuermer CAO. 1988. Retinotopic organization of the developing retinotectal projection in the zebrafish embryo. *J Neurosci* 8:4513–4530.
- Stuermer CAO, Bastmeyer M. 2000. The retinal axon's pathfinding to the optic disk. *Prog Neurobiol* 62:197–214.
- Summerton J. 1999. Morpholino antisense oligomers: the case for an RNase H-independent structural type. *Biochim Biophys Acta* 1489:141–158.
- Thompson JD, Higgins DG, Gibson TJ. 1994. CLUSTAL W: improving the sensitivity of progressive multiple sequence alignment through sequence weighting, position-specific gap penalties and weight matrix choice. *Nucleic Acids Res* 22:4673–4680.
- Uchida N, Yang Z, Combs J, Pourquie O, Nguyen M, Ramanathan R, Fu J, Welplly A, Chen S, Weddell G, Sharma AK, Leiby KR, Karagozeos D, Hill B, Humeau L, Stallcup WB, Hoffman R, Tsukamoto AS, Gearing DP, Peault B. 1997. The characterization, molecular cloning, and expression of a novel hematopoietic cell antigen from CD34+ human bone marrow cells. *Blood* 89:2706–2716.
- Weiland UM, Ott H, Bastmeyer M, Schaden H, Giordano S, Stuermer CAO. 1997. Expression of an L1-related cell adhesion molecule on developing CNS fiber tracts in zebrafish and its functional contribution to axon fasciculation. *Mol Cell Neurosci* 9:77–89.
- Weiner JA, Koo SJ, Nicolas S, Fraboulet S, Pfaff SL, Pourquie O, Sanes JR. 2004. Axon fasciculation defects and retinal dysplasias in mice lacking the immunoglobulin superfamily adhesion molecule BEN/ALCAM/SC1. *Mol Cell Neurosci* 27:59–69.
- Xiao T, Roeser T, Staub W, Baier H. 2005. A GFP-based genetic screen reveals mutations that disrupt the architecture of the zebrafish retinotectal projection. *Development* 132:2955–2967.
- Yamagata M, Sanes JR. 2005. Versican in the developing brain: lamina-specific expression in interneuronal subsets and role in presynaptic maturation. *J Neurosci* 25:8457–8467.
- Yamaguchi M, Tonou-Fujimori N, Komori A, Maeda R, Nojima Y, Li H, Okamoto H, Masai I. 2005. Histone deacetylase 1 regulates retinal neurogenesis in zebrafish by suppressing Wnt and Notch signalling pathways. *Development* 132:3027–3043.